Protein Hydrophobic Collapse and Early Folding Steps Observed in a Microfluidic Mixer

Lisa J. Lapidus,* Shuhuai Yao,[†] Kimberly S. McGarrity,* David E. Hertzog,[†‡] Emily Tubman,* and Olgica Bakajin[†]

*Department of Physics and Astronomy, Michigan State University, East Lansing, Michigan; [†]Chemistry & Material Science Department, Lawrence Livermore National Laboratory, Livermore, California; and [‡]Mechanical Engineering Department, Stanford University, Stanford, California

ABSTRACT   We demonstrate that the sub-millisecond protein folding process referred to as "collapse" actually consists of at least two separate processes. We observe the UV fluorescence spectrum from naturally occurring tryptophans in three well-studied proteins, cytochrome c, apomyoglobin, and lysozyme, as a function of time in a microfluidic mixer with a dead time of ~ 20 μs. Single value decomposition of the time-dependent spectra reveal two separate processes: 1), a spectral shift which occurs within the mixing time; and 2), a fluorescence decay occurring between ~ 100 and 300 μs. We attribute the first process to hydrophobic collapse and the second process to the formation of the first native tertiary contacts.

INTRODUCTION

It has been postulated that hydrophobic collapse, the global contraction of a polypeptide due to mutual attraction of hydrophobic residues, is the first step in folding a protein from a highly denatured state to its native conformation. However, experimental studies in the past have usually been able to only infer collapse from measurements of the burst phase, the unresolved signal change within the dead time of the instrument. The few available time-resolved measurements have reported a wide range of times for collapse. For example, studies on the protein cytochrome c have measured an initial folding step occurring within 100 μs that has been attributed to collapse (1,2), but kinetic measurements of intramolecular contact formation have shown that a simple loop can form in 100 ns to 1 μs, 100–1000 times faster (3,4). Secondary structure may also form on this same timescale, as shown by fast kinetic studies on isolated α-helices and β-hairpins (5), and studies on the unfolded state indicate that fluctuating elements of secondary structure persist even under denaturing conditions (6,7). These observations lead to a chicken-and-egg question of whether the formation of long-range native contacts necessarily requires a commensurate reduction in the overall size of the protein, or does hydrophobic collapse precede the formation of native structure? Our new method to observe folding on faster timescales begins to answer this question by resolving separate steps in the first millisecond of folding.

The current optical techniques used to measure sub-microsecond steps in protein folding, namely laser T-jump, triplet-state quenching, and photophysical dissociation, although great technological advances (8), have all been unable to study collapse of a wide range of proteins because they cannot prompt folding from the fully denatured state. Conversely, stopped-flow mixing, which prompts protein folding from the fully denatured state by the dilution of denaturants, is limited to time resolutions longer than 0.5–1 ms due to turbulence during mixing. Thus, for most proteins, there is a gap in the observable time domain on the microsecond timescale, a crucial time-range for understanding the nature of collapse. In this work, we report the measurement of folding prompted by mixing in a laminar flow microfluidic device that dilutes denaturant in <20 μs and allows observation of intrinsic tryptophan fluorescence, the most common method for observing folding, for as long as 1 ms. Using this technique we have observed three well-studied, unmodified proteins, apomyoglobin, cytochrome c, and lysozyme. We show that for all three proteins there are two separate steps in the first 1 ms. Hydrophobic burial of the tryptophans occurs within the mixing time of 20 μs followed by what we interpret as the formation of native tertiary contacts within ~ 100 and 300 μs. These steps have never been resolved separately before. While the slower process might be considered collapse because the formation of first native contacts requires large conformation changes, we believe that the faster process of nonspecific hydrophobic burial, which requires a large decrease in the radius of gyration, is a better definition of the term.

The proteins used in these studies were chosen because their long-time folding trajectories are very well characterized in measurements with longer mixing times yet these measurements cannot completely resolve the change in the fluorescence signal. Cytochrome c, in particular, has become a benchmark for development of fast folding techniques. The first folding study to employ a microfluidic mixer studied cytochrome c with small angle x-ray scattering (SAXS) and observed a substantial change in the radius of gyration within the first 150–500 μs (9). Akiyama et al. (10) used a similar mixer to measure folding after 300 μs monitored with SAXS and circular dichroism and developed a three-phase model of the folding trajectory:

1. An initial phase of collapse and secondary structure formation that occurs within their mixing time.
2. The formation of a molten globule-like second intermediate after 3 ms.
3. The formation of the native state after 100 ms.

The early phase has been explored by three more rapid measurements: Shastry and Roder (2), using a fast capillary mixer with a dead time of 50 μs, and Hagen and Eaton (1) and Qui et al. (11), each using a 10 ns T-jump. These three measurements observed the initial decrease in fluorescence to occur with decay times of ~50, ~90, and ~16 μs, respectively.

Apomyoglobin also proceeds via a stepwise folding path of chain compaction and helix formation (12), while lysozyme has an off-pathway intermediate (13,14). Nevertheless, both of these proteins, like cytochrome c, have been observed to have a burst phase or unresolved change of signal within the conventional mixing times. During this burst phase, the radius of gyration decreases and the secondary structure content increases. Our major result is that this burst phase appears to actually consist of two processes with rates separated by at least an order of magnitude.

METHODS

Mixer

The basic design of this mixer was first described by Knight et al. (15), and was optimized by Hertzog et al. (16). This design takes advantage of small channel dimensions to keep the dynamics in the laminar flow regime, even for very high velocities, resulting in mixing times of as low as 8 μs. (While the device is capable of mixing times as low as 8 μs, most data was collected with lower flow rates and longer mixing times to achieve a longer observation time. Thus the fastest mixing time observed while also observing folding was 20 μs.) The exit channel is 10-μm wide and 200-μm long. Two-hundred microns below the mixing region the channel widens exponentially allowing for long observation times at high flow rates without substantial diffusion of the protein jet. The fluid dynamics in the chip are simulated with Comsol Multiphysics (Comsol, Stockholm, Sweden). The channels were etched in 500-μm-thick fused silica wafers using reactive ion etching with metal or polysilicon as a mask (see Fig. 1 a). Inlet and outlet holes were microblasted. The channels were then first prebonded to a 170-μm-thick fused silica wafer after a reverse RCA cleaning, and then fused together at 1100°C. The mixer is mounted on a manifold, which contains solution reservoirs for each channel in the chip. The flow rate of each channel is controlled by air pressure above the reservoir using computer-controlled pressure transducers (Marsh Bellofram Type 2000, Newell, WV). At the fastest flow rates reported, the sample consumption is ~2 μL/h of the protein and 400 μL/h of folding buffer. An experiment typically takes ~1 h including setup time.

Optical

The UV fluorescence of a folding protein is monitored with a specially designed confocal microscope (see Fig. 1 b). An Argon-Ion laser (Lexel Laser 95-SHG, Lexington, KY) at 257 nm enters an inverted microscope (Olympus IX51, Melville, NY) as a collimated beam and is focused to a 1 μm spot by a 0.5 NA UV objective (OFR 40x-266, Newton, NJ) inside the mixer. For a linear flow speed of 1 m/s, the 1 μm spot results in a maximum time resolution of 1 μs. Fluorescence intensity is collected by the same objective and sent through a dichroic mirror (Chroma 300dclp, Brattleboro, VT) to either a photon counter (Hamamatsu H7421-40, Hamamatsu City, Japan) or a spectrograph (Jobin Yvon MicroHR, Longjumeau, France) and linear CCD detector (Jobin Yvon Sygnature) with 3648 pixels. The mixer
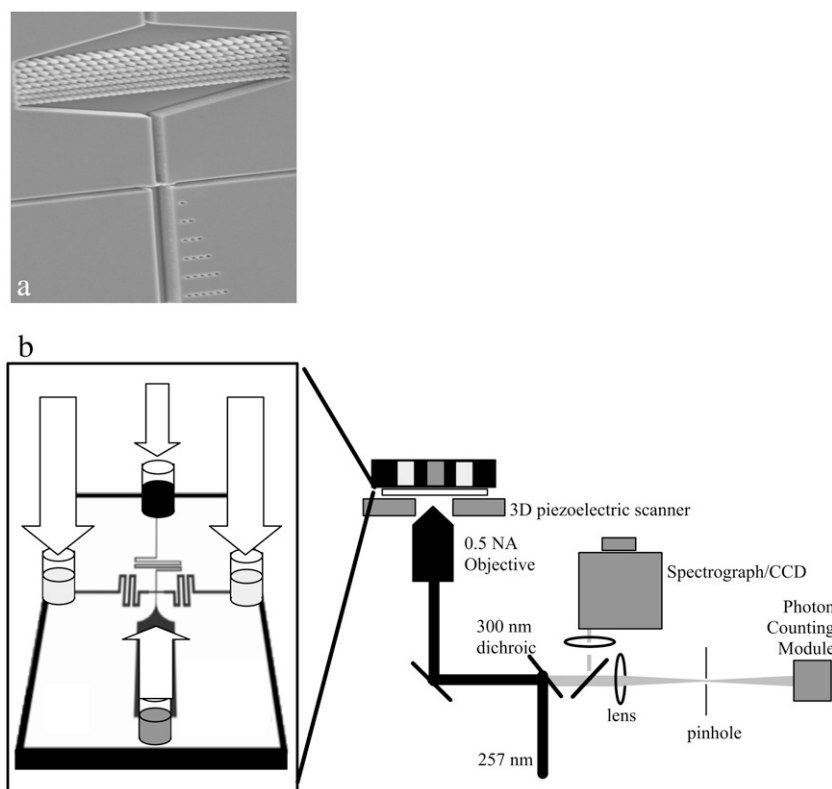

FIGURE 1 (a) Mixing region of chip imaged with a scanning electron microscope. The unfolded protein in the center channel (*top*) passes through a filter of 1-μm posts and enters the mixing region in the center of the image. The mixing buffer enters on the side channels and constricts the protein stream to <100 nm within a few microns of the interaction region. The protein and mixed buffer continue down the 10-μm-wide exit channel for observation during folding. (*b*) Schematic of the instrument. The chip is mated to a manifold containing reservoirs of unfolded protein (*solid*) and buffer (*light shading*), which are pushed into the mixer by computer-controlled air pressure above the reservoirs. The chip sits on a scanning inverted microscope illuminated by 257 nm laser light. The resulting fluorescence is detected by either a photon counter or a spectrograph and CCD camera.

manifold is mounted on a three-axis piezoelectric scanner (Mad City Labs Nano-LP100, Madison, WI), which scans the chip over the objective 100 μm in each direction.

A typical experiment begins with a scan of the exit channel imaged by the photon counter to locate the jet of fluorescent protein (Fig. 2 *a*). The chip is typically scanned 10 μs across the exit channel and 200 μm down the linear section of the exit channel and ~100 μm into the exponentially widening channel. This corresponds to ~320 μs of folding time at an initial flow rate of 1 m/s without substantial diffusion of the protein out of the jet. Alternatively, long time courses can be obtained by slowing the flow rate to as low as 0.1 m/s. The overall intensity as a function of time can be obtained from a scan by averaging the intensity of the jet in ~1 μm regions, the size of the excitation beam (see Fig. 2 *c*).

After the jet in the exit channel has been imaged with the photon counter, the emission is directed to the spectrograph/CCD by inserting a flip-up mirror in the light path. Fluorescence spectra are acquired at numerous points along the jet corresponding to various times from 20 μs to up to 1 ms. Because the mixer is a continuous flow device, each point in the folding trajectory may be observed for an arbitrary amount of time, allowing for a good signal/noise ratio without a particularly fast detector. Spectra are

typically acquired for 1 s at 2-μm intervals along the exit channel (see Fig. 2 *d*). To reduce the noise, the data is binned (10 pixels/bin) to produce spectra with 0.42 nm resolution. The time-dependent spectra are analyzed with single value decomposition using MatLab (The MathWorks, Natick, MA) to extract the most significant time-dependent spectral components.

Protein samples

N-acetyltryptophan-amide (NATA), horse heart cytochrome c, and hen-egg lysozyme were purchased from Sigma (St. Louis, MO) and used without further modification. Horse skeletal muscle myoglobin was also purchased from Sigma. The myoglobin heme was extracted following the method of Teale (18). Proteins were unfolded by dissolving them in high concentrations of Guanidine HCl. Folding was initiated by mixing with 100 mM potassium phosphate buffer (pH 7). The approximate concentrations of each sample were 500 μM cytochrome c, 240 μM apomyoglobin, 90 μM lysozyme, and 500 μM NATA for measurements of time-resolved fluorescence spectra (spectrograph and CCD) and ~10-fold less for measurements of total intensity (photon counting). These concentrations were chosen to give

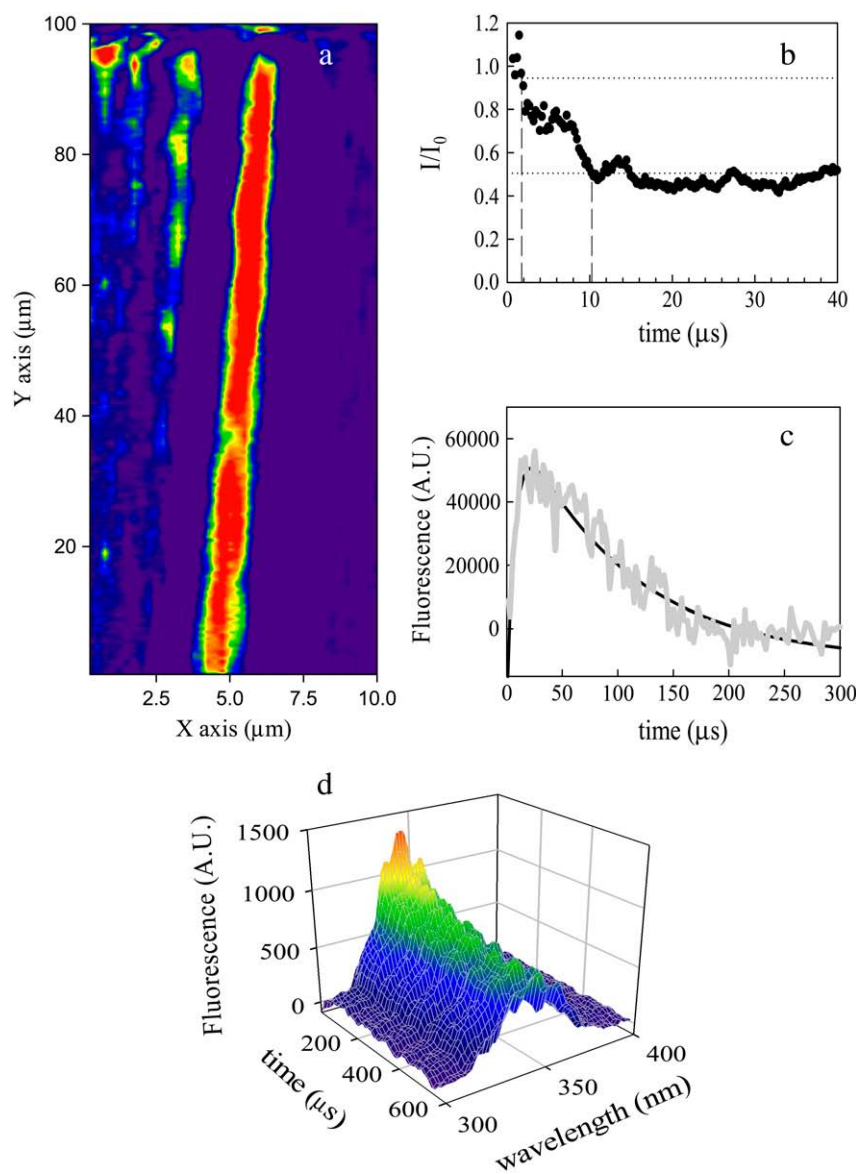FIGURE 2 (*a*) Contour plot of fluorescence intensity of tryptophan (NATA) in the exit channel. The chip was scanned 0.25 μm/step in the x-direction and 0.5 μm/step in the *y*-direction. Each point was observed for 25 ms. We focus the instrument using the fluorescent jet at the bottom of the scan where the index of refraction is that of water. However, the mixing region, located at the top of the plot, has a different index of refraction from the high concentration of GuHCl, which leads to a lack of fluorescence in that region due to the difference in focus. (*b*) Observation of the mixing time with fluorescence quenching by potassium iodide. Plotted is the ratio of intensity of NATA fluorescence in 150 mM KI to no KI versus time. The mixing time, defined as the time during which the signal decays from 90% to 10% (*dotted lines*) of the premixed value, is ~8 μs. (*c*) Observation of fluorescence (via photon counting) from cytochrome c in folding conditions. The initial rise in intensity ($\tau \sim 13$ μs) is due to the change in the index of refraction during mixing. The longer decay ($\tau \sim 100$ μs) is due to the first step in folding. (*d*) Time-resolved fluorescence spectra of cytochrome c (measured by the spectrograph/CCD). A global analysis of this type of data using single value decomposition produces the curves in Fig. 3.

about the same fluorescence signal for each protein. While these concentrations of protein may eventually lead to aggregation, it is unlikely on the timescales observed because the bimolecular diffusion rate for these proteins is $\sim 10^8 \, M^{-1} \, s^{-1}$ and aggregation is not diffusion-limited. Furthermore, other folding experiments on these proteins have worked with similar concentrations without detecting aggregation (9,13,19).

RESULTS

Using continuous-flow microfluidic mixers made out of fused silica (see Fig. 1 a), we are for the first time able to observe changes in tryptophan fluorescence with 20 μs mixing time. The mixing time is determined by measuring the drop in average NATA fluorescence due to quenching by potassium iodide (150 mM) in the exit channel (see Fig. 2 b). The mixing time can also be observed as a rise in fluorescence intensity after the dilution of guanidine due to a change in the index of refraction (Fig. 2 c). The measured mixing times (8 and 13 μs, respectively) are in good agreement with previously reported values (16).

Fig. 2 c shows total photon intensity as a function of time for cytochrome c; the decay rate agrees reasonably well with the measurements of Shastry and Roder (2). Photon counting is a very sensitive measurement, which can observe the fluorescence of tryptophan concentrations as low as 20 μM. However, measuring the total intensity is also sensitive to background artifacts due to scattered laser light and is completely insensitive to changes in the fluorescence spectrum that do not affect the fluorescence quantum yield. Therefore, fluorescence spectra were collected along the exit channel using the spectrograph/CCD (see Fig. 2 d). This method effectively eliminates all background effects because scattered light is spectrally separated from the fluorescence, and allows for a global analysis of time resolved and spectrally resolved fluorescence.

Fig. 3 shows the time-resolved spectral data of each protein analyzed with single value decomposition (SVD) to suppress the random noise of each spectrum. For all three proteins, the first component is the average emission spectrum over the measured time domain. The first component (*solid points*) can be fit to two exponentials—a fast decay due to the narrowing of the jet in the mixing region and a slow decay on the 100-μs timescale. The second component shows the change in spectrum over time. The amplitude of the spectral shift (*shaded points*) decays over time with a rate approximately equal to the mixing time as measured by tryptophan fluorescence quenching by potassium iodide.

We observe that the decay rate of the second component depends on the overall flow rate as shown in Fig. 3. The relative flow rate between the center and side channels determines the mixing distance in the exit channel and the faster flow rate of the side channel determines the mixing time. To confirm that this rate is the actual mixing time, we performed fluid dynamics simulations of mixing at various flow rates of the side channels with a constant flow rate ratio

to the center channel. These rates, shown as a line in Fig. 4, agree well with the measured values and confirm that the spectral shift occurs within the mixing time. This puts an upper limit on this process of 20 μs.

DISCUSSION

This work observes, for the first time, folding on the microsecond timescale using spectrally resolved intrinsic fluorescence. Surprisingly, we see very similar behavior in three completely unrelated proteins. We attribute the blue spectral shift observed within the mixing time (*shaded curves* in Fig. 3) for all three proteins to hydrophobic burial of the tryptophan resulting from global collapse (20). A similar measurement of NATA in 6 M GuHCl (Fig. 3 h) shows that free tryptophan does not exhibit a significant spectral shift on this timescale, indicating that this process is not merely a solvent or optical effect. To further confirm that this process occurs only during mixing, Fig. 4 shows the fitted rate of the second SVD component of lysozyme plotted versus flow rate, indicating that the rate of spectral shift is limited by the mixing time. Because the entire process occurs within the mixing time of this experiment, we assign an upper limit of 20 μs for the hydrophobic burial and for the collapse of the polypeptide chain. Of course, the data only directly reports on the hydrophobic burial of individual residues, but we believe these signals are representative of the behavior of the entire polypeptide chain, particularly in the case of lysozyme, which has six tryptophans distributed throughout the sequence.

We note that our measurement of hydrophobic collapse is consistent with other measurements of collapse. Roder and colleagues observed an increase in tryptophan fluorescence intensity of ribonuclease A within their 70 μs mixing time and attributed it to nonspecific collapse (21). Measurements of intramolecular diffusion in unstructured peptides indicate that diffusion-limited intramolecular contact should take between 20 and 500 ns for loops between 10 and 60 residues (22,23). Furthermore, measurements of end-to-end distance after a rapid temperature-jump in acid-denatured BBL, a 40-residue protein, showed that hydrophobic collapse was complete in only 80 ns at room temperature (24). This time is likely the result of the formation of many small loops within the chain rather than a single loop formed by the two ends and is therefore quite consistent with the intramolecular contact measurements. Given these estimates of intramolecular diffusion during hydrophobic collapse, the mixing time of our apparatus would likely need to improve by two orders of magnitude to fully resolve this process.

The slower process that we observed (*solid curves* in Fig. 3) shows no spectral change for each protein, only decay in the blue-shifted spectrum. There are many interactions that have been shown to decrease the level of tryptophan fluorescence including changes in solvent conditions, but our
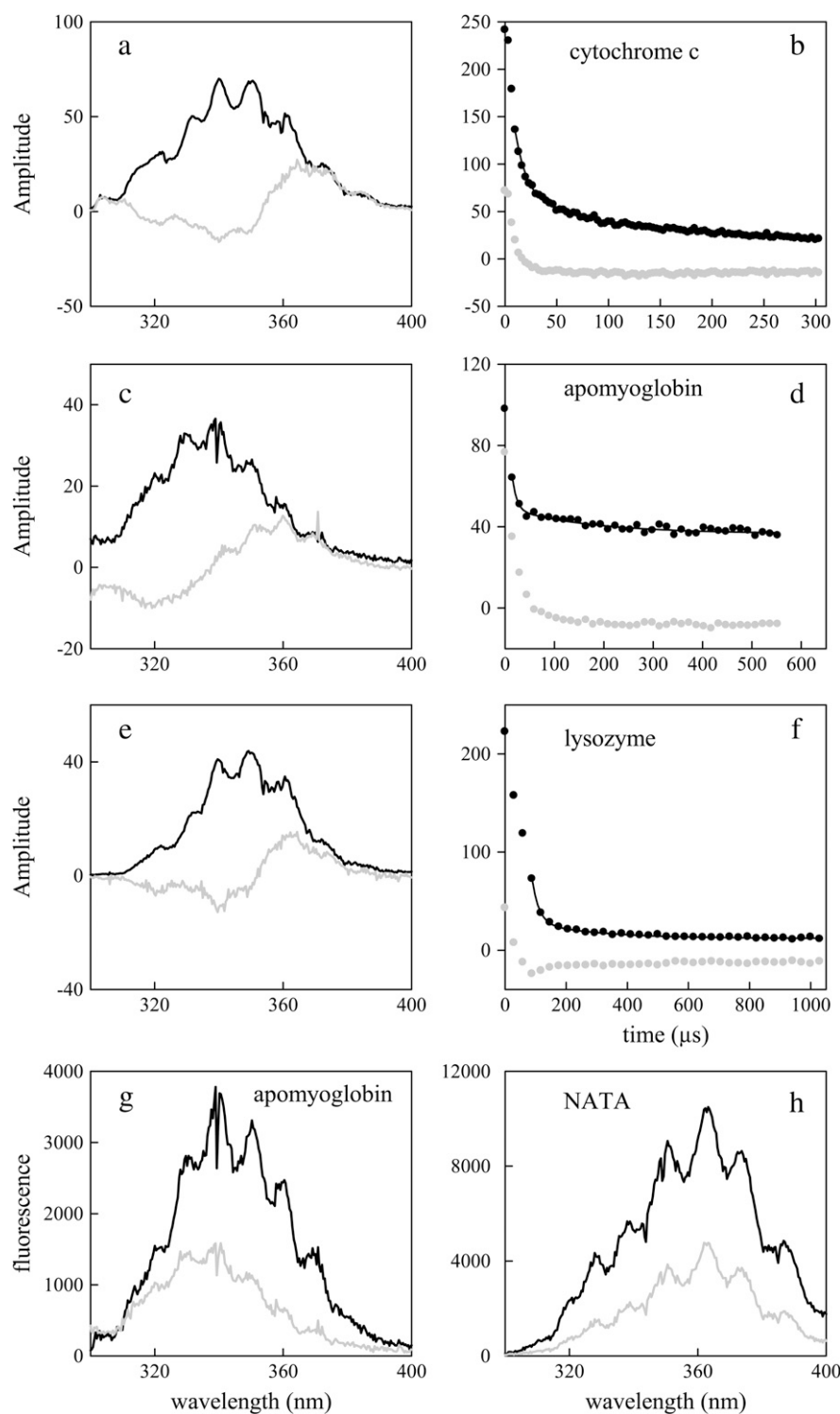
FIGURE 3 (a–f) Time-dependent fluorescence spectra analyzed with single value decomposition. The left panels are the most significant spectral components and the right panels are the associated time dependence. For all three proteins, the first component (solid) is the average spectrum whose intensity decays during mixing due to formation of the jet and on the 100-μs timescale, and the second component (shading) is a difference spectrum between the unfolded state and the folded state that decays only within the mixing time. The flow rates, 0.6 m/s (cytochrome c), 0.14 m/s (apomyoglobin), and 0.068 m/s (lysozyme), were chosen to capture multiple decay times of the slow process for each protein. The time dependence of the first component (solid points) is fit to two exponentials for determining the rates in Fig. 5, ignoring the first three or four points in the mixing decay because it is not truly exponential. (g, h) Raw fluorescence of apomyoglobin (g) and NATA (h). The black curves were observed just above the mixing region and the shaded curves observed 10 μm below the mixing region (when mixing is complete) to compare the spectral shift in a folding protein with that of free tryptophan.

characterization of this mixer rules out a solvent effect after the mixing time of 20 μs (16). Therefore, we attribute this process to the formation of tertiary contacts near the tryptophan, which quench the fluorescence. Previous studies have shown that there is structural evidence to support the observed decrease of tryptophan fluorescence for each of these proteins on the 100-μs timescale:

1. The two tryptophan residues in apomyoglobin (Trp-7 and Trp-14) are located on the A helix in the native structure and are in close contact with the E and H and E and G helices, respectively. Hydrogen exchange studies have determined that the native folding core consisting of the A, G, and H helices is formed early in the folding process (25). Therefore our observed decrease in fluorescence in
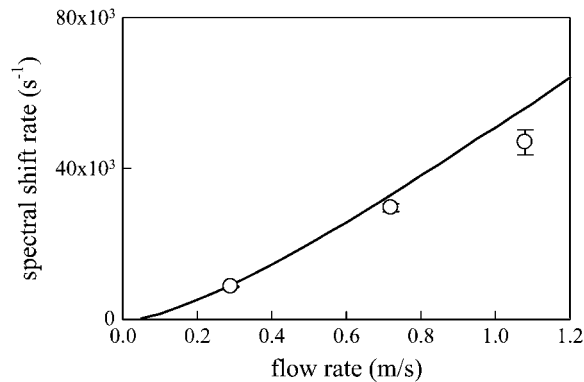
FIGURE 4   Plot of observed rates (*circles*) of the second SVD component of lysozyme as a function of the flow rate in the exit channel. The amplitude of this component was fit to a single exponential as a function of distance. The characteristic distance is converted to time using a simulated distance-time relation. The solid line is the simulated mixing rate for maximum velocities of 0.05–1.2 m/s in the exit channel. The mixing time is calculated as the elapsed time at the location along each streamline where the GuHCl concentration drops from 1 to $1/e$. These values are averaged for all the streamlines within the confocal beam diameter of 1 μm (38).

$\sim$225 μs probably corresponds to the docking of the A helix with helices G and H. Our result is corroborated by a kinetic study of apomyoglobin fluorescence using T-jump, which shows a large signal change of 7 μs followed by a very small change on the 100–500 μs timescale (19).

2. Fast hydrogen exchange studies on lysozyme suggest that some protection of residues throughout the helical domain and at the interface of the α- and β-domains (including most of the six tryptophan residues), but that these structures are not completely nativelike (26). Therefore our signal change in $\sim$250 μs reflects the formation of various native contact throughout the chain.

3. It has been well established that the single tryptophan in cytochrome c acts as a donor in fluorescence energy transfer with the heme (2). Hydrogen exchange studies show some protection of the three main helices, but not Trp-59 early in the folding process. However, it is likely that the formation of the nativelike helical interactions pulls the tryptophan fairly close to the heme without making a native contact (27). A recent study combining single molecule FRET and fluorescence correlation spectroscopy concludes that the intermediate structure of cytochrome c is compact but largely unstructured in the middle of the chain (28). Therefore the decrease in tryptophan fluorescence observed in $\sim$100 μs is due to the formation of some native contacts within the chain, but not the tryptophan itself.

Thus the evidence for all three proteins supports our conclusion that the slow phase marks the formation of long-range contacts and that these contacts are likely nativelike.

While the slower rate obviously depends on the details of the folding trajectory of each protein, we note that all three measured rates anticorrelate well with the fraction of secondary structure formed. In studies by Bachmann et al.
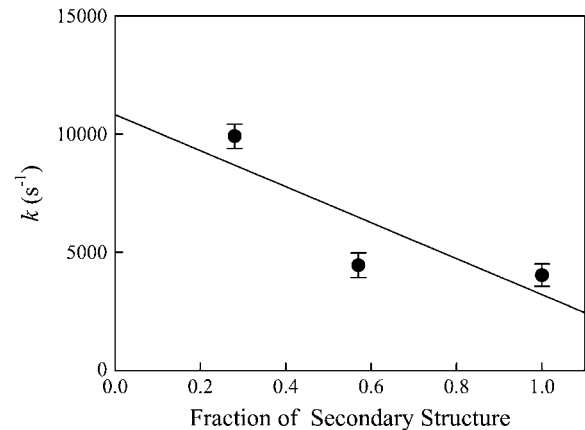

FIGURE 5   Rates of fluorescence quenching versus formation of secondary structure in the burst phase as measured with slower mixers. The fractions of secondary structure are taken from the literature (12,13,29) and are computed as the change in CD signal between the unfolded value and the first measurable value over the total change in CD between the unfolded and folded states. The rates are weighted averages of three-to-four measurements of each protein. Each measurement was in a different chip except for one chip, which measured all three proteins. The numeric values of the rates are (cytochrome c) 9903 $\pm$ 515 s^{-1}, (apomyoglobin) 4449 $\pm$ 518 s^{-1}, and (lysozyme) 4028 $\pm$ 475 s^{-1}.

(13) on lysozyme, Akiyama et al. (10) on cytochrome c, and Uzawa et al. (12) on apomyoglobin, the amount of secondary structure that formed within their mixing times (0.3–1.2 ms) were measured using time-resolved circular dichroism. The studies by Bachmann and Uzawa and another study by Akiyama (29) also show a significant decrease in the radius of gyration, as measured by small angle x-ray scattering (SAXS), during these dead times. The fraction of secondary structure formed in their dead times is plotted versus our measured rates of tryptophan fluorescence decay in Fig. 5. This correlation ($r = 0.71$) is significantly better than the correlation of the rates with relative contact order ($r = 0.27$). This trend is also consistent with observations by Roder and co-workers of ACBP, ribonuclease A, staphylococcal nuclease, and Im7. The first three proteins have a measured fluorescence decay of $\sim$12,000 s^{-1} (21,30,31) and fairly small amounts of secondary structure ($<$33%) formed within 1 ms (32–34), while Im7 has a measured fluorescence decay of $\sim$3000 s^{-1} (35) and likely all of its secondary structure formed (36). The correlation suggests that it is easier to make the first long-range stabilizing contacts if there is relatively little secondary structure formed that would slow down intramolecular diffusion. Whether the initial secondary structure content forms in the fast or slow processes observed in our mixer cannot be determined from these studies and would be the subject of future work, such as time-resolved circular dichroism after ultrarapid mixing (37). Nevertheless, it is clear that this new technique opens up an entirely new time domain to reveal protein-folding steps never seen before.

REFERENCES

1. Hagen, S. J., and W. A. Eaton. 2000. Two-state expansion and collapse of a polypeptide. *J. Mol. Biol.* 301:1019–1027.

2. Shastry, M. C. R., and H. Roder. 1998. Evidence for barrier-limited protein folding kinetics on the microsecond time scale. *Nat. Struct. Biol.* 5:385–392.

3. Buscaglia, M., B. Schuler, L. J. Lapidus, W. A. Eaton, and J. Hofrichter. 2003. Kinetics of intramolecular contact formation in a denatured protein. *J. Mol. Biol.* 332:9–12.

4. Lapidus, L. J., W. A. Eaton, and J. Hofrichter. 2000. Measuring the rate of intramolecular contact formation in polypeptides. *Proc. Natl. Acad. Sci. USA.* 97:7220–7225.

5. Kubelka, J., J. Hofrichter, and W. A. Eaton. 2004. The protein folding ''speed limit''. *Curr. Opin. Struct. Biol.* 14:76–88.

6. Kazmirski, S. L., K.-B. Wong, S. M. V. Freund, Y.-J. Tan, A. R. Fersht, and V. Daggett. 2001. Protein folding from a highly disordered denatured state: the folding pathway of chymotrypsin inhibitor 2 at atomic resolution. *Proc. Natl. Acad. Sci. USA.* 98:4349–4354.

7. Hodsdon, M. E., and C. Frieden. 2001. Intestinal fatty acid binding protein: the folding mechanism as determined by NMR studies. *Biochemistry.* 40:732–742.

8. Eaton, W. A., V. Munoz, S. J. Hagen, G. S. Jas, L. J. Lapidus, E. R. Henry, and J. Hofrichter. 2000. Fast kinetics and mechanisms in protein folding. *Annu. Rev. Biophys. Biomol. Struct.* 29:327–359.

9. Pollack, L., M. W. Tate, N. C. Darnton, J. B. Knight, S. M. Gruner, W. A. Eaton, and R. H. Austin. 1999. Compactness of the denatured state of a fast-folding protein measured by submillisecond small-angle x-ray scattering. *Proc. Natl. Acad. Sci. USA.* 96:10115–10117.

10. Akiyama, S., S. Takahashi, K. Ishimori, and I. Morishima. 2000. Stepwise formation of alpha-helices during cytochrome *c* folding. *Nat. Struct. Biol.* 7:514–520.

11. Qiu, L. L., C. Zachariah, and S. J. Hagen. 2003. Fast chain contraction during protein folding: ''foldability'' and collapse dynamics. *Phys. Rev. Lett.* 90:168103.

12. Uzawa, T., S. Akiyama, T. Kimura, S. Takahashi, K. Ishimori, I. Morishima, and T. Fujisawa. 2004. Collapse and search dynamics of apomyoglobin folding revealed by submillisecond observations of alpha-helical content and compactness. *Proc. Natl. Acad. Sci. USA.* 101:1171–1176.

13. Bachmann, A., D. Segel, and T. Kiefhaber. 2002. Test for cooperativity in the early kinetic intermediate in lysozyme folding. *Biophys. Chem.* 96:141–151.

14. Segel, D. J., A. Bachmann, J. Hofrichter, K. O. Hodgson, S. Doniach, and T. Kiefhaber. 1999. Characterization of transient intermediates in lysozyme folding with time-resolved small-angle x-ray scattering. *J. Mol. Biol.* 288:489–499.

15. Knight, J. B., A. Vishwanath, J. P. Brody, and R. H. Austin. 1998. Hydrodynamic focusing on a silicon chip: mixing nanoliters in microseconds. *Phys. Rev. Lett.* 80:3863–3866.

16. Hertzog, D. E., X. Michalet, M. Jager, X. X. Kong, J. G. Santiago, S. Weiss, and O. Bakajin. 2004. Femtomole mixer for microsecond kinetic studies of protein folding. *Anal. Chem.* 76:7169–7178.

17. Reference deleted in proof.

18. Teale, F. W. J. 1959. Cleavage of the haem-protein link by acid methylethylketone. *Biochim. Biophys. Acta.* 35:543.

19. Ballew, R. M., J. Sabelko, and M. Gruebele. 1996. Direct observation of fast protein folding: the initial collapse of apomyoglobin. *Proc. Natl. Acad. Sci. USA.* 93:5759–5764.

20. Lakowicz, J. R. 1999. Principles of Fluorescence Spectroscopy. Plenum, New York.

21. Welker, E., K. Maki, M. C. R. Shastry, D. Juminaga, R. Bhat, H. A. Scheraga, and H. Roder. 2004. Ultrarapid mixing experiments shed new light on the characteristics of the initial conformational ensemble during the folding of ribonuclease a. *Proc. Natl. Acad. Sci. USA.* 101:17681–17686.

22. Krieger, F., B. Fierz, O. Bieri, M. Drewello, and T. Kiefhaber. 2003. Dynamics of unfolded polypeptide chains as model for the earliest steps in protein folding. *J. Mol. Biol.* 332:265–274.

23. Lapidus, L. J., P. J. Steinbach, W. A. Eaton, A. Szabo, and J. Hofrichter. 2002. Effects of chain stiffness on the dynamics of loop formation in polypeptides. Appendix: testing a one-dimensional diffusion model for peptide dynamics. *J. Phys. Chem. B.* 106:11628–11640.

24. Sadqi, M., L. J. Lapidus, and V. Munoz. 2003. How fast is protein hydrophobic collapse? *Proc. Natl. Acad. Sci. USA.* 100:12117–12122.

25. Jennings, P. A., and P. E. Wright. 1993. Formation of a molten globule intermediate early in the kinetic folding pathway of apomyoglobin. *Science.* 262:892–896.

26. Gladwin, S. T., and P. A. Evans. 1996. Structure of very early protein folding intermediates: new insights through a variant of hydrogen exchange labeling. *Fold. Des.* 1:407–417.

27. Sauder, J. M., and H. Roder. 1998. Amide protection in an early folding intermediate of cytochrome c. *Fold. Des.* 3:293–301.

28. Werner, J. H., R. Joggerst, R. B. Dyer, and P. M. Goodwin. 2006. A two-dimensional view of the folding energy landscape of cytochrome c. *Proc. Natl. Acad. Sci. USA.* 103:11130–11135.

29. Akiyama, S., S. Takahashi, T. Kimura, K. Ishimori, I. Morishima, Y. Nishikawa, and T. Fujisawa. 2002. Conformational landscape of cytochrome *c* folding studied by microsecond-resolved small-angle x-ray scattering. *Proc. Natl. Acad. Sci. USA.* 99:1329–1334.

30. Maki, K., H. Cheng, D. A. Dolgikh, M. C. R. Shastry, and H. Roder. 2004. Early events during folding of wild-type staphylococcal nuclease and a single-tryptophan variant studied by ultrarapid mixing. *J. Mol. Biol.* 338:383–400.

31. Teilum, K., K. Maki, B. B. Kragelund, F. M. Poulsen, and H. Roder. 2002. Early kinetic intermediate in the folding of acyl-COA binding protein detected by fluorescence labeling and ultrarapid mixing. *Proc. Natl. Acad. Sci. USA.* 99:9807–9812.

32. Kimura, T., S. Akiyama, T. Uzawa, K. Ishimori, I. Morishima, T. Fujisawa, and S. Takahashi. 2005. Specifically collapsed intermediate in the early stage of the folding of ribonuclease A. *J. Mol. Biol.* 350:349–362.

33. Sugawara, T., K. Kuwajima, and S. Sugai. 1991. Folding of staphylococcal nuclease-A studied by equilibrium and kinetic circular-dichroism spectra. *Biochemistry.* 30:2698–2706.

34. Teilum, K., B. B. Kragelund, J. Knudsen, and F. M. Poulsen. 2000. Formation of hydrogen bonds precedes the rate-limiting formation of persistent structure in the folding of ACBP. *J. Mol. Biol.* 301:1307–1314.

35. Capaldi, A. P., M. C. R. Shastry, C. Kleanthous, H. Roder, and S. E. Radford. 2001. Ultrarapid mixing experiments reveal that im7 folds via an on-pathway intermediate. *Nat. Struct. Biol.* 8:68–72.

36. Spence, G. R., A. P. Capaldi, and S. E. Radford. 2004. Trapping the on-pathway folding intermediate of im7 at equilibrium. *J. Mol. Biol.* 341:215–226.

37. Hoffman, A., A. Kane, D. Nettles, D. E. Hertzog, P. Baumgartel, J. Lengefeld, G. Reichardt, D. A. Horsley, R. Seckler, O. Bakajin, and B. Schuler. 2007. Mapping protein collapse with single-molecule fluorescence and kinetic synchrotron radiation circular dichroism spectroscopy. *Proc. Natl. Acad. Sci. USA.* 104:105–110.

38. Park, H. Y., X. Y. Qiu, E. Rhoades, J. Korlach, L. W. Kwok, W. R. Zipfel, W. W. Webb, and L. Pollack. 2006. Achieving uniform mixing in a microfluidic device: Hydrodynamic focusing prior to mixing. *Anal. Chem.* 78:4465–4473.